

# High-resolution observations of interstellar Na I and Ca II towards the southern opening of the ‘Local Interstellar Chimney’: probing the disc–halo connection

I. A. Crawford,<sup>1\*</sup> R. Lallement,<sup>2</sup> R. J. Price,<sup>1</sup> D. M. Sfeir,<sup>3,4</sup>  
B. P. Wakker<sup>5</sup> and B. Y. Welsh<sup>3</sup>

<sup>1</sup>*Department of Physics and Astronomy, University College London, Gower Street, London WC1E 6BT*

<sup>2</sup>*Service d’Aéronomie du CNRS, BP 3, 91371 Verrieres-le-Buisson, France*

<sup>3</sup>*Space Sciences Laboratory, University of California, Berkeley, CA 94720, USA*

<sup>4</sup>*Department of Aerospace and Mechanical Engineering, University of Southern California, Los Angeles, CA 90089, USA*

<sup>5</sup>*Department of Astronomy, University of Wisconsin, 475 N. Charter Street, Madison, WI 53706, USA*

Accepted 2002 August 9. Received 2002 August 7; in original form 2002 July 12

## ABSTRACT

We present high-resolution ( $R = 400\,000$ ) observations of interstellar Ca II and Na I absorption lines towards seven stars in the direction of the southern opening of the recently identified Local Interstellar Chimney. These lines of sight probe the lower Galactic halo ( $0.3 \lesssim |z| \lesssim 2.5$  kpc), without the complication of sampling dense foreground interstellar material. In addition to components with velocities expected from Galactic rotation, these stars also exhibit components with negative local standard of rest velocities, which are contrary to the sense of Galactic rotation for the sightlines observed. After a discussion of possible origins for these peculiar velocities, we conclude that at least some of them result from gas falling towards the Galactic plane from distances of  $|z| \gtrsim 300$  pc. The narrow linewidths are generally inconsistent with temperatures as high as the  $\sim 6000$  K generally assumed for the so-called Lockman layer. Rather, the picture that emerges is one of a scattered, generally infalling, population of high- $|z|$  diffuse clouds, seemingly not very different from those encountered in the local interstellar medium. Overall, we argue that our results are most consistent with a ‘Galactic fountain’ model.

**Key words:** ISM: structure – Galaxy: halo.

## 1 INTRODUCTION

As part of an on-going programme to explore the structure of the local interstellar medium by means of high-resolution absorption-line spectroscopy (e.g. Crawford, Craig & Welsh 1997; Crawford, Lallement & Welsh 1998), we report here on a study of interstellar Ca II K and Na I D lines towards seven stars situated in the lower Galactic halo ( $0.3 \lesssim |z| \lesssim 2.5$  kpc). Our aim is to study the physical and kinematical state of matter in the lower halo, and its relationship to more local interstellar structures in the solar vicinity.

It is generally accepted (e.g. Cox & Reynolds 1987; Frisch 1995), that the Sun is situated within a hot ( $T \sim 10^6$  K), low-density ( $n_{\text{H}} \sim 0.005$  cm $^{-3}$ ) region known as the local bubble (LB). Recently, Sfeir et al. (1999) have conducted a preliminary survey of Na I absorption within 300 pc of the Sun, and revealed the presence of an ab-

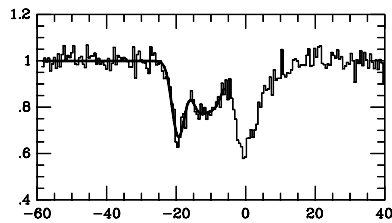
sorption boundary (or ‘wall’) of cold, and relatively dense [ $N(\text{H I}) > 5 \times 10^{19}$  cm $^{-2}$ ] neutral gas surrounding the LB at distances from the Sun varying between 65 and 250 pc. This neutral boundary of the LB is found to be well defined in the Galactic plane, but at high Galactic latitudes the LB appears to be open-ended in both hemispheres with no well-defined dense neutral absorption boundary. This ‘Local Interstellar Chimney’ (a term first coined by Welsh et al. 1999) is found to point towards  $l = 155^\circ$ ,  $b = +58^\circ$ , to extend at least to  $|z| \approx 200$  pc and to be tilted perpendicularly to the plane of Gould’s Belt. The presence of this open-ended structure provides a unique opportunity to probe the structure of the inner halo region by means of high-resolution measurements of interstellar absorption lines that are essentially free from the interference of dense foreground clouds.

The neutral inner halo is thought to consist of a confined, cool ( $T \lesssim 500$  K) component with an exponential scaleheight of  $\sim 100$  pc (where the interstellar medium largely forms discrete clouds), and

\*E-mail: iac@star.ucl.ac.uk

an extended, more rarefied warm ( $T \sim 6000$  K; e.g. Spitzer & Fitzpatrick 1993) diffuse component with an estimated scaleheight of  $\sim 500$  pc (the so-called 'Lockman layer'; Lockman 1984; Lockman, Hobbs & Shull 1986). Although the latter was originally envisaged as a smooth distribution of 'intercloud' type material (Lockman et al. 1986), more recent work suggests an interpretation where the whole H I layer consists of essentially discrete clouds, the individual motions of which support its vertical extent against the Galactic gravitational potential (Lockman & Gehman 1991 and references therein). This latter interpretation is supported by the extensive survey of Albert et al. (1993), which found evidence for discrete clouds (as mapped by Ca II and Ti II absorption lines) at distances  $\gtrsim 1$  kpc above and below the plane.

Further away from the Galactic disc the halo gas is thought to be highly ionized (the so-called 'Reynolds layer', Reynolds 1997 and references therein; see also de Boer 1998), although the proposed 1-kpc scaleheight sits uncomfortably with the apparent detection of discrete, presumably largely neutral, clouds at and beyond this distance from the plane by Albert et al. (1993). Moreover, given the existence of this ionized component, it is still uncertain whether the hot ionized gas is being advected from the disc into the halo by a



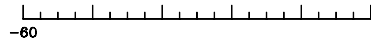
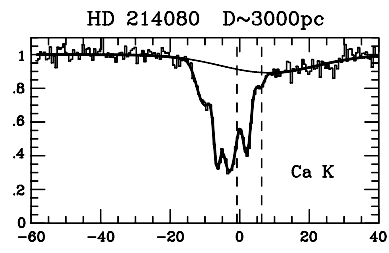


**Table 1.** List of stellar and observational data. The visual magnitudes ( $V$ ), spectral types, and Galactic coordinates ( $l$ ,  $b$ ) are taken from the SIMBAD data base. (The question mark for the spectral type of HD 210191 flags an uncertainty discussed in Section 3).  $E_{B-V}$  is the colour excess, calculated from the observed colours and the intrinsic colours listed by Schmidt-Kaler (1982);  $D_{\text{Hipp}}$  and  $D_{\text{phot}}$  are the *Hipparcos* trigonometric (ESA 1997) and photometric distances, respectively, both rounded to the nearest two significant figures (the photometric distances assume the absolute magnitudes given by Schmidt-Kaler 1982).  $W_{\lambda}(\text{Ca K})$  and  $W_{\lambda}(\text{Na D}_2)$  are the total interstellar Ca K and Na D<sub>2</sub> equivalent widths, respectively. The last two columns indicate the number and length of integrations made in each spectral region.

Star (HD)	$V$	Sp. Type	$l$	$b$	$D_{\text{Hipp}}$ (pc)	$D_{\text{phot}}$ (pc)	$E_{B-V}$	$W_{\lambda}(\text{Ca K})$ (mÅ)	$W_{\lambda}(\text{Na D}_2)$ (mÅ)	Exp. (Ca II) ( $n \times s$ )	Exp. (Na I) ( $n \times s$ )
208213	8.5	B3 Vn	17.90	-51.47	$610^{+1100}_{-240}$	1010	0.04	$94 \pm 4$	$7 \pm 4$	$2 \times 1800$	$1 \times 1800$
209522	6.0	B4 IVne	23.58	-53.01	$350^{+120}_{-70}$	390	0.04	$50 \pm 2$	$32 \pm 2$	$1 \times 1200$	$2 \times 1200$
210191	5.8	B2 III ?	37.15	-51.76	$2100^{+\infty}_{-1400}$	770	0.08	$83 \pm 2$	$102 \pm 2$	$2 \times 1200$	$1 \times 1800$
213728	6.7	B7 III	14.99	-59.87	$360^{+150}_{-80}$	400	0.06	$9 \pm 2$	$< 3.5$	$4 \times 1200$	$1 \times 1800$
214080	6.8	B1/2 Ib	44.80	-56.92	$3700^{+\infty}_{-2800}$	3110	0.05	$104 \pm 3$	$213 \pm 2$	$4 \times 1200$	$1 \times 1800$
219639	6.6	B5 II/III	54.81	-65.63	$610^{+1100}_{-240}$	790	0.07	$35 \pm 3$	$68 \pm 2$	$4 \times 1200$	$1 \times 1800$ $2 \times 600$
219833	7.2	A0 V	63.04	-63.68	$520^{+480}_{-170}$	200	0.03	$8 \pm 2$	$35 \pm 3$	$3 \times 1800$	$1 \times 1800$

dispersion ( $b$ ) and column density ( $N$ ). The best-fitting profiles, following convolution with the instrumental response function ( $b_{\text{inst}} \equiv 0.75/1.6651 = 0.45 \text{ km s}^{-1}$ ), are shown superimposed on the data in Fig. 1, and the resulting line-profile parameters are listed in Table 2.

### 3 STELLAR DISTANCES AND RELATION TO THE ‘CHIMNEY’

Clearly, the interpretation of the observed absorption-line profiles depends crucially on the stellar distances. Unfortunately, there is considerable uncertainty in the distances of several of these stars, as all but three lie well beyond the  $\sim 500$ -pc limit of *Hipparcos* (at which distance the median precision of the measured parallaxes,  $\Delta\pi \approx 1$  mas, amounts to about 50 per cent of the trigonometrical parallax, ESA 1997). For this reason, Table 1 also lists the photometrically derived distances, based on the published spectral types. Such distances are, of course, also notoriously unreliable, depending critically on the assumed spectral type (and especially the luminosity class). There is general agreement between the photometric and *Hipparcos* distances, given the errors, but in some cases the uncertainties are still so large that this comparison is of little help. For consistency within the present study, we have chosen tentatively to adopt the *Hipparcos* distances (rounded to the nearest 50 pc where appropriate) for the five stars where this is  $\lesssim 600$  pc. The adopted distances for all the stars are listed with the appropriate panels in Fig. 1. Only in the case of HD 208213 is this value very different from the photometric estimate. For the more distant star HD 214080 both the photometric and *Hipparcos* values suggest a distance of  $\sim 3$  kpc, and we will adopt that here.

In the case of HD 210191 (35 Aqr), there is a large disparity in the distance estimates and little independent evidence to decide between them. However, we may note that a distance as low as 350 pc, adopted by Lockman et al. (1986) on the basis of a B2.5 IV spectral type, is now excluded by the *Hipparcos* parallax. Matters are further complicated by an apparent ambiguity concerning the spectral type of this star. While that adopted here (B2 III) is derived from the generally reliable Michigan Catalogue (Houk & Smith-Moore 1988), and is similar to earlier determinations (e.g. B2 IV, Lesh 1968), the

fact is that a spectral type as early as this makes it difficult to account for the observed strengths of the photospheric Ca K and Na D lines (Fig. 1).

While the strengths of the photospheric lines towards the other stars are generally consistent with the adopted spectral types, trial solar-metallicity LTE atmospheric modelling conducted using the spectrum synthesis code UCLSYN (Smith 1992) suggests an effective temperature of  $\sim 11\,000$  K (i.e. a spectral type  $\sim \text{B8/9}$ ) to account for the observed photospheric lines for HD 210191. Indeed, at B2 the photospheric Na D lines would not be expected to be detectable, and this region should instead be dominated by the C II 5889.78 Å-line (e.g. Crawford 1990), which is not observed. On the other hand, it is also true that a spectral type as late as B9 III results in a distance (only 190 pc) that is effectively excluded by the *Hipparcos* measurement. While the atmospheric modelling, particularly of the Ca line, provided some indication that  $\log g$  might also be very low ( $\sim 2.5$ ), indicative of supergiant status and a distance of  $\sim 1600$  pc (which is consistent with the *Hipparcos* measurement), it is clear that a much more careful analysis of the stellar spectrum will be needed to solve this particular puzzle. For the moment we tentatively adopt a distance of  $\sim 1$  kpc for HD 210191 as a compromise between the photometric and *Hipparcos* values, but note that this is very uncertain.

From the Galactic coordinates listed in Table 1 it can be seen that four of the seven stars (HD 208213, 209522, 210191 and 213728) lie within  $\lesssim 10^\circ$  of a plane perpendicular to the Galactic plane and directed towards  $l = 25^\circ$ . Fig. 2(a) shows a slice through the ‘Local Chimney’ along this plane, produced using the method developed by Sfeir et al. (1999), and the projected locations of these four stars. It is clear that all four are located in the direction of the southern end of the Chimney, but at distances greater than the stars used to define it. Fig. 2(b) shows a similar diagram for the remaining three stars (HD 214080, 219639 and 219833), where the slice through the Chimney lies in the direction  $l = 55^\circ$  (where, again, the stars lie within  $\lesssim 10^\circ$  of this plane).

Fig. 3 shows the locations of the stars with respect to the low-velocity ( $-50 \leq v_{\text{LSR}} \leq +50 \text{ km s}^{-1}$ ) H I distribution mapped by Hartmann & Burton (1997). From this we see that the total low-velocity H I column density towards the observed stars generally lies in the range  $2 \pm 1 \times 10^{20} \text{ cm}^{-2}$ . Clearly, it is of interest to determine

**Table 2.** Line profile parameters for the interstellar Ca K and Na D<sub>2</sub> lines towards the observed stars. The last column gives the Na I/Ca II column density ratio. Because two well-defined Na I components towards HD 219639 are observed to correspond to a broader, more poorly defined, Ca II feature, the later has been modelled as two component with velocities fixed to the Na I values; these are indicated by asterisks (but note that the  $-11.1 \text{ km s}^{-1}$  Ca component is barely significant).

Star (HD)	Ca K			Na D <sub>2</sub>			$N(\text{Na I})/N(\text{Ca II})$
	$v_{\text{LSR}}$ ( $\text{km s}^{-1}$ )	$b$ ( $\text{km s}^{-1}$ )	$N (\times 10^{10})$ ( $\text{cm}^{-2}$ )	$v_{\text{LSR}}$ ( $\text{km s}^{-1}$ )	$b$ ( $\text{km s}^{-1}$ )	$N (\times 10^{10})$ ( $\text{cm}^{-2}$ )	
208213	$-19.3 \pm 0.3$	$2.3 \pm 0.3$	$25.5 \pm 0.8$	....	....	$\leq 3.0$	$\leq 0.12$
	$-13.3 \pm 3.0$	$3.2 \pm 1.0$	$19.8 \pm 2.9$	....	....	$\leq 3.0$	$\leq 0.18$
	$-8.6 \pm 3.7$	$3.2 \pm 1.0$	$16.9 \pm 2.2$	....	....	$\leq 3.0$	$\leq 0.20$
	$-0.8 \pm 0.4$	$2.7 \pm 0.6$	$37.2 \pm 1.2$	$-0.6 \pm 0.5$	$1.6 \pm 0.7$	$3.9 \pm 3.2$	$0.11 \pm 0.09$
	$+2.9 \pm 0.6$	$1.7 \pm 0.8$	$11.7 \pm 0.2$	....	....	$\leq 3.0$	$\leq 0.26$
	$+7.2 \pm 1.2$	$3.2 \pm 1.5$	$9.6 \pm 4.8$	....	....	$\leq 3.0$	$\leq 0.63$
209522	$-18.4 \pm 0.1$	$2.1 \pm 0.2$	$9.9 \pm 0.7$	$-18.6 \pm 0.3$	$1.3 \pm 0.4$	$1.4 \pm 0.8$	$0.14 \pm 0.08$
	$-14.8 \pm 0.3$	$0.8 \pm 0.5$	$1.6 \pm 0.3$	....	....	$\leq 0.7$	$\leq 0.54$
	$-11.2 \pm 0.3$	$2.3 \pm 0.6$	$8.2 \pm 0.6$	$-12.2 \pm 0.4$	$2.6 \pm 0.6$	$3.4 \pm 1.2$	$0.42 \pm 0.15$
	....	....	$\leq 1.4$	$-9.2 \pm 0.1$	$0.5 \pm 0.2$	$3.1 \pm 1.9$	$\geq 0.86$
	$-5.6 \pm 0.6$	$3.7 \pm 0.8$	$10.4 \pm 0.6$	$-6.3 \pm 0.1$	$0.6 \pm 0.2$	$2.5 \pm 1.3$	$0.24 \pm 0.13$
	$+2.5 \pm 0.1$	$1.6 \pm 0.1$	$33.2 \pm 2.7$	$+2.3 \pm 0.2$	$2.7 \pm 0.2$	$5.4 \pm 0.1$	$0.16 \pm 0.02$
210191	$-21.8 \pm 0.1$	$1.6 \pm 0.1$	$40.3 \pm 2.7$	$-21.7 \pm 0.1$	$1.16 \pm 0.03$	$16.0 \pm 2.2$	$0.40 \pm 0.06$
	$-16.1 \pm 0.1$	$1.6 \pm 0.1$	$61.3 \pm 3.7$	$-16.0 \pm 0.1$	$1.11 \pm 0.02$	$55.3 \pm 1.9$	$0.90 \pm 0.06$
	$-8.2 \pm 0.1$	$2.5 \pm 0.2$	$15.9 \pm 0.1$	....	....	$\leq 0.5$	$\leq 0.03$
	$+2.0 \pm 0.1$	$0.9 \pm 0.1$	$9.2 \pm 1.8$	$+2.0 \pm 0.1$	$0.67 \pm 0.07$	$8.0 \pm 1.5$	$0.87 \pm 0.24$
	....	....	$\leq 1.8$	$+4.5 \pm 0.4$	$1.4 \pm 0.5$	$1.4 \pm 0.5$	$\geq 0.50$
	$+6.8 \pm 0.2$	$2.2 \pm 0.4$	$6.2 \pm 0.2$	....	....	$\leq 0.5$	$\leq 0.08$
213728	$-12.8 \pm 0.2$	$2.5 \pm 0.3$	$7.3 \pm 1.9$	....	....	$\leq 0.8$	$\leq 0.15$
	$+14.0 \pm 0.3$	$2.5 \pm 0.5$	$5.3 \pm 1.9$	....	....	$\leq 0.8$	$\leq 0.24$
214080	$-10.0 \pm 0.3$	$2.9 \pm 0.4$	$24.3 \pm 5.6$	$-10.2 \pm 0.1$	$0.44 \pm 0.21$	$1.8 \pm 0.1$	$0.07 \pm 0.02$
	$-6.4 \pm 0.1$	$1.0 \pm 0.2$	$27.6 \pm 8.5$	$-5.3 \pm 0.1$	$1.28 \pm 0.04$	$490 \pm 59^\dagger$	$17.8 \pm 5.9$
	$-2.9 \pm 0.1$	$2.6 \pm 0.3$	$79.4 \pm 14.0$	$-2.1 \pm 0.1$	$1.90 \pm 0.09$	$94.6 \pm 7.2$	$1.19 \pm 0.23$
	$+2.1 \pm 0.1$	$1.4 \pm 0.2$	$32.0 \pm 6.0$	$+3.1 \pm 0.1$	$0.84 \pm 0.05$	$23.3 \pm 2.5$	$0.73 \pm 0.16$
	$+5.9 \pm 0.4$	$1.4 \pm 0.6$	$4.4 \pm 3.1$	$+5.8 \pm 0.2$	$1.74 \pm 0.21$	$10.0 \pm 2.9$	$2.27 \pm 1.73$
219639	$-11.1^*$	$1.8 \pm 0.8$	$3.9 \pm 3.8$	$-11.1 \pm 0.2$	$1.2 \pm 0.3$	$1.8 \pm 0.8$	$0.46 \pm 0.49$
	$-8.1^*$	$2.5 \pm 0.8$	$8.6 \pm 4.8$	$-8.1 \pm 0.1$	$1.3 \pm 0.1$	$9.3 \pm 1.0$	$1.08 \pm 0.61$
	$-3.0 \pm 0.1$	$0.9 \pm 0.1$	$24.1 \pm 5.8$	$-3.2 \pm 0.1$	$1.57 \pm 0.03$	$34.3 \pm 1.3$	$1.42 \pm 0.35$
	$-0.4 \pm 0.2$	$1.1 \pm 0.3$	$9.8 \pm 3.9$	$+0.8 \pm 0.1$	$0.85 \pm 0.14$	$2.1 \pm 0.7$	$0.21 \pm 0.11$
219833	$-7.5 \pm 0.2$	$1.1 \pm 0.3$	$7.9 \pm 1.6$	$-7.2 \pm 0.1$	$1.2 \pm 0.2$	$8.7 \pm 2.5$	$1.10 \pm 0.39$
	$-3.0 \pm 0.2$	$1.7 \pm 0.4$	$9.6 \pm 1.9$	$-3.6 \pm 0.4$	$2.5 \pm 0.5$	$10.0 \pm 2.7$	$1.04 \pm 0.35$

\*Ca II velocities fixed at Na I values; see the table caption.

<sup>†</sup>Note that this component is fully saturated in Na D<sub>2</sub> and  $N$  is constrained by the weaker D<sub>1</sub> line; however, as D<sub>1</sub> itself reaches a residual intensity of just 1 per cent, the resulting  $N$  is uncertain and should probably be viewed as a lower limit.

whether the present observations of absorption lines are able to place limits on the distance to this H I. Na I is often used as a tracer for hydrogen in the diffuse interstellar medium, and Ferlet, Vidal-Madjar & Gry's (1985) relationship implies that (with the notable exception of HD 214080) much of the H I mapped at 21 cm lies beyond the stars. Unfortunately, Ferlet et al.'s relation actually displays considerable scatter, and suffers from order-of-magnitude uncertainties at low  $[N(\text{Na I}) \lesssim 10^{11} \text{ cm}^{-2}]$  column densities (e.g. Welty et al. 1994; Wakker & Mathis 2000). However, even allowing for this uncertainty, it does appear that at least in the cases of HD 208213 and 213728 [for which the Ferlet et al. relation predicts  $N(\text{H I}) \sim 8 \times 10^{18}$  and  $\lesssim 4 \times 10^{18} \text{ cm}^{-2}$ , respectively] the bulk of the H I lies in the background (i.e. at distances  $\gtrsim 500$  pc). This is rather further than expected from the notional extent of the Lockman layer, but quite consistent with the greater scaleheights found for Ca II and Ti II by Albert et al. (1993). Finally, we note that while the one

star with a significantly greater Na I (and thus inferred H) column density, HD 214080, is also the most distant, Fig. 1 indicates that most of this is contributed by a single, strong velocity component at  $v_{\text{LSR}} = -5.3 \text{ km s}^{-1}$ , presumably a result of a dense interstellar cloud relatively close to the Sun (and perhaps associated with the Chimney boundary; cf. Fig. 2b).

## 4 DISCUSSION

### 4.1 The velocity structure

Much of the interpretation of the present data hinges on the radial velocities of the observed interstellar absorption components. Thus, after a brief discussion of the stellar radial velocities and possible *circumstellar* absorption, we will discuss how the observed velocities relate to those expected from Galactic rotation and

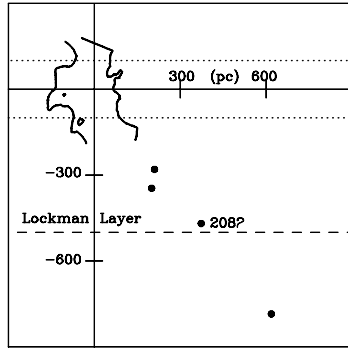


**Table 3.** The LSR radial velocity ranges expected to arise from Galactic rotation [ $v_{\text{LSR}}$  (Galaxy)] and, where appropriate, the near (–) and far (+) sides of the expanding Loop II bubble [ $v_{\text{LSR}}$  (Loop II)] towards the observed stars. The next two columns give the stellar radial velocities, where  $v_{\text{LSR}}^*$  (SIMBAD) are the published values on the SIMBAD data base (where available), and  $v_{\text{LSR}}^*$  (Here) are the values obtained here from the observed stellar Ca K and Na D lines. The number in the last column ( $\Delta v_{\text{helio}}^{\text{LSR}}$ ) should be *added* to the LSR velocities to give the heliocentric values.

Star (HD)	$v_{\text{LSR}}$ (Galaxy) (km s <sup>–1</sup> )	$v_{\text{LSR}}$ (Loop II) (km s <sup>–1</sup> )	$v_{\text{LSR}}^*$ (SIMBAD) (km s <sup>–1</sup> )	$v_{\text{LSR}}^*$ (Here) (km s <sup>–1</sup> )	$\Delta v_{\text{helio}}^{\text{LSR}}$ (km s <sup>–1</sup> )
208213	–0.4 to +1.4	....	–64.8	....	–2.2
209522	–0.5 to +0.5	....	....	....	–2.3
210191	–0.8 to +3.8	±6.6	–1.8	–8.1 (Ca) –12.0 (Na)	–3.4
213728	–0.3 to +0.4	....	....	–20.7 (Ca) +3.5 (Na)?	+0.1
214080	–0.8 to +6.3	±9.1	+2.2	+8.4 (Ca)	–2.2
219639	–0.7 to +0.4	±10.1	....	–13.4 (Ca)	+0.2
219833	–0.8 to +5.9	±11.8	....	+5.7 (Ca)	–0.3

obtain the projected line-of-sight velocities given in Table 3, and these are indicated by vertical dashed lines in Fig. 1. For all the stars discussed here, even the very distant HD 214080, the radial velocity resulting from Galactic rotation increases almost linearly with distance. Thus, of the velocity range delineated in Fig. 1, the lower boundary corresponds to local material, essentially at rest with respect to the LSR. The upper limits are then the velocities predicted at the adopted stellar distances. We note that the velocity range expected to arise from Galactic rotation is much more restricted at these high Galactic latitudes than it would be in the plane, owing to the strong latitude dependence (e.g. Cohen 1975).

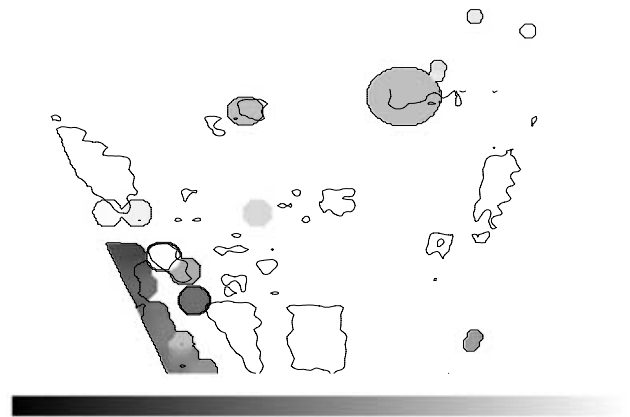
It is apparent from Fig. 1 that most of these stars do have absorption components within, or at least close to (i.e. within  $\sim 5$  km s<sup>–1</sup>), the velocity range expected from Galactic rotation. However, it is notable that they all also exhibit absorption components outside this range, and in all cases except the +14 km s<sup>–1</sup> component towards HD 213728 these occur at more *negative* velocities. It is important to realize that, for stars in this Galactic longitude range and at these distances, significant negative LSR velocities are contrary to the sense of Galactic rotation, and so must arise from some other cause. This tendency for high Galactic latitude absorption to exhibit peculiar velocities with respect to a halo corotating with the disc has, in fact, already been noted in several earlier studies (e.g. Albert et al. 1993, and references therein). Note, that while Albert et al. identified examples of *positive* peculiar velocities towards two of the present stars (HDs 210191 and 214080), the higher resolution employed here enables us to identify these with the red wings of the photospheric lines (compare the relevant panels of our Fig. 1 with their fig. 2). Thus, in the present sample all the peculiar interstellar velocities (with the single exception of the weak +14 km s<sup>–1</sup> Ca II component towards HD 213728) are negative, and we now turn to a discussion of possible explanations for them.

#### 4.1.3 Interstellar bubbles

A common origin of high-velocity, especially high negative velocity, interstellar absorption components are the expanding shells and bubbles associated with OB associations [first discussed by Münch (1957), and subsequently studied by many other authors; see Crawford, Barlow & Blades (1989) for a brief summary]. Although these structures are generally located close to the Galactic plane, this being the location of the OB associations responsible for them, it is possible in principle for even quite high-latitude lines of sight to

penetrate relatively nearby shells that subtend large angular sizes on the sky. This possibility is graphically illustrated by Gahm (1994) who has compiled a list of all the known interstellar bubbles within 1 kpc, several of which extend to  $|b| \gtrsim 60^\circ$ .

However, it turns out that the only known interstellar bubble in the foreground to the stars observed here is the very large non-thermal radio continuum structure known as Loop II (otherwise known as the Cetus Arc; e.g. Large, Quigley & Haslam 1962; Berkhuijsen 1973; Vallée 1994). Indeed, we find that these seven stars actually straddle the Loop II boundary. Given the well-determined Loop II centre ( $l = 100^\circ$ ,  $b = -32.5^\circ$ ), Fig. 4 shows the extent of this feature on the sky, for both a radius of  $45^\circ$ , which is the radius of peak emission, and the larger ‘half-power’ radius of  $53^\circ$  obtained by Berkhuijsen (1973), which we take to be a conservative upper limit for its maximum extent. We see that HD 208213, 209522 and 213728 certainly



lie outside Loop II on the sky, and HD 214080, 219639, 219833 certainly lie within it; HD 210191 lies close to the boundary, but lies just within it if we adopt the larger radius given by Berkhuijsen (1973). Following Gahm (1994) and adopting this larger size, the projected LSR radial velocities for the near and far sides of Loop II for the four stars found within it are given in Table 3, where we have adopted an expansion velocity of  $19 \text{ km s}^{-1}$  (Vallée 1994). It is immediately apparent that while Loop II might, in principle, account for low negative velocity ( $v_{\text{LSR}} \approx -10 \text{ km s}^{-1}$ ) absorption towards HD 214080, 219639 and 219833, it cannot plausibly account for the highest blueshifted velocities observed here ( $v_{\text{LSR}} \lesssim -15 \text{ km s}^{-1}$ ). Given the high Galactic latitudes, it is unlikely that more distant, as yet unrecognized, OB association bubbles exist in the foreground to these stars.

#### 4.1.4 High-velocity clouds

In principle, highly blueshifted (or redshifted) interstellar absorption lines at high Galactic latitudes could be associated with the high- and intermediate-velocity clouds (HVCs and IVCs, respectively) detected in 21-cm H I surveys (e.g. Wakker & van Woerden 1997; Wakker 2001 and references therein). Although the distances that have been estimated to-date for a relatively small number of HVCs and IVCs would lead us to expect them to lie well beyond the stars observed here, it is nevertheless of interest to determine whether the current observations can yield any useful information concerning such structures in this direction.

The total velocity coverage of the present spectra, of which only a small part is shown in Fig. 1, was  $-350$  to  $+200 \text{ km s}^{-1}$  for Ca K, and  $-450$  to  $+100 \text{ km s}^{-1}$  for Na D<sub>1</sub> (Na D<sub>2</sub> extending to only  $-130 \text{ km s}^{-1}$  owing to the placement of the doublet on the detector). No velocity components were detected in either species within these velocity ranges, other than the low-velocity components shown in Fig. 2. Depending only slightly on the signal-to-noise ratios of the individual spectra, these non-detections imply Na I column density limits of  $\lesssim 10^{10} \text{ cm}^{-2}$  for any HV gas that may be present. The corresponding H I limits, based on the relationship of Ferlet et al. (1985) are then  $\lesssim 10^{18} \text{ cm}^{-2}$  (but note the order-of-magnitude uncertainty on this relationship discussed in Section 3).

Fig. 4 shows the distribution of HVC and IVC structures in the direction of the stars observed here (Bajaja et al. 1985; Hulsbosch & Wakker 1988; Morras, Bajaja & Pöppel 2000). Unfortunately, there are only a few coincidences in position between the stars and the HV/IV clouds, limiting the conclusions that can be drawn. HD 219639 does project on to an IVC and the absence of corresponding Na I absorption (with the limits given in Table 3) may imply a distance  $\gtrsim 600 \text{ pc}$  for this cloud. However, as discussed by Wakker (2001), it is important to realize that this conclusion depends on the assumption of detectable column densities being present within the IVC, which, for a given line of sight, may also depend on the degree of clumping in the cloud (e.g. Shaw et al. 1996). In this case, if the Na I and Ca II abundances were at the low end of values typically found for IVCs, or if the sightline passed between clumps, then this one might not have been detected here even if it were closer than the star. Similarly, the lack of IV absorption towards HD 213728 may imply a distance  $\gtrsim 400 \text{ pc}$  for the IVC close to its position (although in this case the positional coincidence is not exact).

## 4.2 Evidence for infall?

Summarizing the above, it seems clear that neither the foreground Loop II shell, or the background HVC/IVC complexes, can account

for the moderately negative velocity absorption ( $-25 \lesssim v_{\text{LSR}} \lesssim -10 \text{ km s}^{-1}$ ) observed towards HDs 208213, 209522 and 210191. While in no sense extreme by interstellar standards, the fact that these velocities are contrary to the sense of Galactic disc rotation implies that they represent a different kinematical component, presumably in the lower halo, or material that is falling towards the Galactic plane from higher  $z$ .

The three stars that exhibit these components all lie fairly close together on the sky (cf. Figs 4 and 2a), and a broadly co-spatial origin at a distance  $\lesssim 350 \text{ pc}$  (the distance to the nearest star of the three) may be implied. On the other hand, although the uncertainties in the stellar distances make it hard to be definitive (Table 1), it seems that while the gross velocity structure is similar, the *strengths* of the lines in this velocity range increase with distance. Moreover, strong Na I lines are present in this velocity range towards HD 210191 (at  $\sim 1 \text{ kpc}$ ) that are absent for the nearer stars. These considerations actually argue against a purely local ( $\lesssim 350 \text{ pc}$ ) location for this material, and instead suggest that the lower halo gas in this direction occupies a common velocity range ( $-25 \lesssim v_{\text{LSR}} \lesssim -10 \text{ km s}^{-1}$ ). In this interpretation weak components, similar to those towards the nearer stars, would also be present towards HD 210191, but masked by stronger absorption arising from more distant gas sharing the same infall velocity.

These three stars lie in areas 22 (HD 210191) and 23 (HDs 208213 and 209522) defined by Albert et al. (1993) in their study of halo structure. Albert et al. observed several other stars in each of these areas (cf. their table 1), which may in principle be used to constrain the closest distance to which this blueshifted material approaches the Galactic plane. It turns out that no absorption components in the velocity range of interest here were detected towards any of the other (five) stars in these areas excluding the present three. With the exception of the very distant ( $\sim 4 \text{ kpc}$ ) HD 206144 (where the relevant velocity range is obscured by blending with a stronger low-velocity component), the *Hipparcos* parallaxes (ESA 1997) all yield distances of approximately  $200 \text{ pc}$ . Thus the non-detection of anomalous blueshifted components towards these stars by Albert et al. (1993) may imply a lower limit of  $200 \text{ pc}$  for the closest infalling material in this direction (although it would of course be desirable to repeat the study of Albert et al. with the same spectral resolution as employed here to confirm this conclusion).

Fig. 4 shows that HDs 208213, 209522 and especially HD 210191, all lie close to high-velocity gas associated with WW627. Although the velocities are lower than the corresponding H I emission ( $\sim -135 \text{ km s}^{-1}$ ), it is interesting to note that Kalberla et al. (1997) have recently drawn attention to what they call ‘velocity bridges’ of H I, which seem to connect a number of HVCs with low-velocity material. Further studies may therefore be warranted to determine whether the ‘common infall’ velocities observed here in the general direction of WW627 represent a detection of the same phenomenon in optical absorption lines. Clearly, should such a physical connection be demonstrated, it would imply an interaction between HVCs and the lower halo, with possibly far-reaching implications for our understanding of halo structure. Note that some limits may be placed on the spatial extent of this infall region by noting the absence of absorption in this velocity range towards HD 213 728 and 214080. Clearly, the observation of many more stars in this area of sky, and at a range of distances, will be required to confirm the existence of a discrete region displaying common infall velocities, and to check for any connection with the (presumably background) HVC WW627.



### 4.3 The $b$ -values

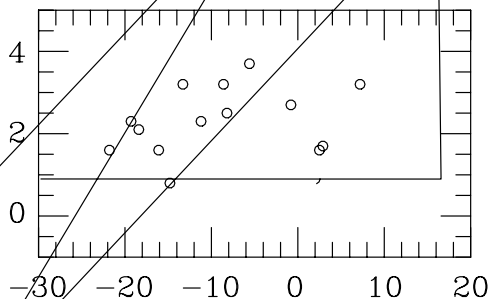
The primary line-broadening mechanisms in the neutral interstellar medium are thermal Doppler broadening and broadening caused by bulk motions of the gas ('turbulence'). These combine to produce an observed velocity dispersion,  $b$ , as follows:

$$b = \sqrt{\frac{2kT_k}{m_A} + 2v_t^2}, \quad (1)$$

where  $T_k$  is the kinetic temperature,  $v_t$  is the line-of-sight turbulent velocity,  $k$  is Boltzmann's constant and  $m_A$  is the mass of the element (atomic mass  $A$ ) under observation. This equation can be used to place constraints on the physical conditions of the absorbing medium. In particular, by setting  $v_t = 0$  it is possible to use an observed  $b$ -value to obtain a rigorous upper limit to the kinetic temperature,  $T_k^{\text{ul}}$ .

One of the primary aims of the present project was to exploit the extremely high resolving power of the UHRF to search for evidence of broader than usual interstellar lines towards these high-latitude stars. This is of particular interest for the more distant objects, where the lines of sight should probe the warm/hot 'Lockman' and 'Reynolds' layers, and where warmer and/or more turbulent gas might be expected. Indeed, some previous work (e.g. Danly 1989) has claimed the detection of very broad ( $b \approx 100 \text{ km s}^{-1}$ ) absorption lines towards halo stars, but it now appears more likely that these extreme widths result from the failure to resolve all the velocity components in the line of sight. For example, on the basis of *IUE* data, Danly (1989) found interstellar absorption with a FWHM of  $\sim 50 \text{ km s}^{-1}$  (centred at  $v_{\text{LSR}} \sim 0 \text{ km s}^{-1}$ ) towards HD 214080, but the present observations (Fig. 1, Table 2) reveal no less than five discrete absorption components in this velocity range (note that the difficulty of resolving this structure in the UV results not only from the lower resolution employed, but also from the intrinsically much stronger lines).

Fig. 5 shows the  $b$ -values obtained here plotted as a function of LSR velocity, and it is clear that, while there is a certain amount of scatter, the values for individual clouds are all quite modest. On the other hand, it is true that the median  $b$ -values ( $2.10 \text{ km s}^{-1}$  for Ca II and  $1.28 \text{ km s}^{-1}$  for Na I) are somewhat larger than the values typically found for comparably well-resolved clouds closer to the Galactic plane. For example, the extensive Ca II survey of Welty, Morton & Hobbs (1996) found a median Ca II  $b$ -value of  $1.31 \text{ km s}^{-1}$ , while the companion Na I survey of Welty et al. (1994) found a median Na I  $b$ -value of  $0.73 \text{ km s}^{-1}$ . Thus, there is some evidence





clouds, not unlike those commonly found in the local interstellar medium (i.e. with relatively cool interiors surrounded by warmer and/or more turbulent haloes), which extends for many hundreds of parsecs above the plane. However, for the bias towards infall (already noted by many previous authors), this would support the modified view of the H I distribution advanced by Lockman & Gehman (1991), where the extent of the neutral medium is maintained by the motions of individual clouds within the Galactic gravitational potential. However, as already noted by Lockman & Gehman, the apparent lack of *redshifted* halo components strongly implies that the *outflowing* gas does not exist in the same form. Overall, then, our observations seem most consistent with the ‘Galactic fountain’ model of Shapiro & Field (1976), where hot, fully ionized, gas rises into the halo as a fountain, but descends in the form of neutral clouds such as those observed here.

## ACKNOWLEDGMENTS

We thank PATT for the award of telescope time, and Elly Berkhuysen for helpful correspondence on the structure of Loop II. IAC and RJP thank PPARC for the awards of an Advanced Fellowship and a Research Studentship, respectively.

## REFERENCES

- Abt H.A., Cardona O., 1984, *ApJ*, 285, 190  
 Albert C.E., Blades J.C., Morton D.C., Lockman F.J., Proulx M., Ferrarese L., 1993, *ApJS*, 88, 81  
 Barlow M.J., 1978, *MNRAS*, 183, 417  
 Bajaja E. et al., 1985, *ApJS*, 58, 143  
 Berkhuysen E.M., 1973, *A&A*, 24, 143  
 Bertin P., Lallement R., Ferlet R., Vidal-Madjar A., 1993, *A&A*, 278, 549  
 Bregman J., Harrington J., 1986, *ApJ*, 309, 833  
 Cardelli J.A., Federman S.R., Smith V.V., 1991, *ApJ*, 381, L17  
 Centurion M., Vladilo G., 1991, *ApJ*, 372, 494  
 Cohen J.G., 1975, *ApJ*, 197, 117  
 Cox D.P., Reynolds R.J., 1987, *ARA&A*, 25, 303  
 Crawford I.A., 1990, *Observatory*, 110, 145  
 Crawford I.A., 1992, *MNRAS*, 259, 47  
 Crawford I.A., 2001a, *MNRAS*, 327, 841  
 Crawford I.A., 2001b, *MNRAS*, 328, 1115  
 Crawford I.A., Barlow M.J., Blades J.C., 1989, *ApJ*, 336, 212  
 Crawford I.A., Craig N., Welsh B.Y., 1997, *A&A*, 317, 889  
 Crawford I.A., Lallement R., Welsh B.Y., 1998, *MNRAS*, 300, 1181  
 Danly L., 1989, *ApJ*, 342, 785  
 de Boer K.S., 1998, *LNP*, 506, 433  
 Diego F., 1993, *Appl. Opt.*, 32, 6284  
 Diego F. et al., 1995, *MNRAS*, 272, 323  
 ESA, 1997, *The Hipparcos and Tycho Catalogues*, ESA SP-1200  
 Ferlet R., Vidal-Madjar A., Gry C., 1985, *ApJ*, 298, 838  
 Fich M., Blitz L., Stark A.A., 1989, *ApJ*, 342, 272  
 Frisch P.C., 1995, *Space Sci. Rev.*, 72, 499  
 Gahm G.F., 1994, *Baltic Astron.*, 3, 85  
 Gardiner L.T., Noguchi M., 1996, *MNRAS*, 278, 191  
 Hartmann D., Burton W.B., 1997, *Atlas of Galactic Neutral Hydrogen*. Cambridge Univ. Press, Cambridge  
 Hobbs L.M., 1976, *ApJ*, 206, L117  
 Hobbs L.M., Wallerstein G., Hu E.M., 1982, *ApJ*, 252, L17  
 Hobbs L.M., Vidal-Madjar A., Ferlet R., Albert C.E., Gry C., 1985, *ApJ*, 293, L29  
 Holweger H., Hempel M., Kamp I., 1999, *A&A*, 350, 603  
 Houk N., Smith-Moore M., 1988, *Michigan Catalogue of Two-Dimensional Spectral Types for the HD Stars*, Vol. 4. Univ. of Michigan, Ann Arbor  
 Howarth I.D., Murray J., Mills D., Berry D.S., 1998, *Starlink User Note*, 50.21  
 Hulsbosch A.N.M., Wakker B.P., 1988, *A&AS*, 75, 191  
 Jura M., 1976, *ApJ*, 206, 691  
 Kalberla P.M.W., Westphalen G., Pietz J., Mebold U., Hartmann D., Burton W.B., 1997, in Lesch H., Dettmar R.-J., Mebold U., Schlickeiser R., eds, *The Physics of Galactic Halos*. Akademie Verlag, Berlin, p. 57  
 Lallement R., Bertin P., Chassefiere E., Scott N., 1993, *A&A*, 271, 734  
 Large M.I., Quigley M.J.S., Haslam C.G.T., 1962, *MNRAS*, 124, 405  
 Lesh J.R., 1968, *ApJS*, 17, 371  
 Lockman F.J., 1984, *ApJ*, 283, 90  
 Lockman F.J., Gehman C.S., 1991, *ApJ*, 382, 182  
 Lockman F.J., Hobbs L.M., Shull J.M., 1986, *ApJ*, 301, 380  
 Morras R., Bajaja E., Pöppel W.G.I., 2000, *A&AS*, 142, 25  
 Morton D.C., 1991, *ApJS*, 77, 119  
 Münch G., 1957, *ApJ*, 125, 42  
 Phillips A.P., Pettini M., Gondhalekar P.M., 1984, *MNRAS*, 206, 337  
 Pottasch S.R., 1972, *A&A*, 20, 245  
 Reynolds R.J., 1997, in Lesch H., Dettmar R.-J., Mebold U., Schlickeiser R., eds, *The Physics of Galactic Halos*. Akademie Verlag, Berlin, p. 57  
 Routly P.M., Spitzer L., 1952, *ApJ*, 115, 227  
 Savage B., Sembach K., 1996, *ApJ*, 457, 211  
 Schmidt-Kaler T.H., 1982, in Schaifers K., Voigt H.H., eds, *Landolt-Börnstein, Numerical Data and Functional Relationships in Science and Technology*. Group VI, Astronomy, Astrophysics and Space Research, Vol. 2b. Springer-Verlag, Berlin  
 Sfeir D.M., Lallement R., Crifo F., Welsh B.Y., 1999, *A&A*, 346, 785  
 Shapiro P.R., Field G.B., 1976, *ApJ*, 205, 762  
 Shaw C.R., Bates B., Kemp S.N., Keenan F.P., Davies R.D., Roger R.S., 1996, *ApJ*, 473, 849  
 Shortridge K. et al., 1998, *Starlink User Note*, 86.16  
 Siluk R.S., Silk J., 1974, *ApJ*, 192, 51  
 Smith K.C., 1992, PhD thesis, Univ. London  
 Spitzer L., 1990, *ARA&A*, 28, 71  
 Spitzer L., Fitzpatrick E.L., 1993, *ApJ*, 409, 299  
 Vallée J.P., 1994, *A&SS*, 220, 243  
 Vallerga J.V., Vedder P.W., Craig N., Welsh B.Y., 1993, *ApJ*, 411, 729  
 Wakker B.P., 2001, *ApJS*, 136, 463  
 Wakker B.P., Mathis J.S., 2000, *ApJ*, 544, L107  
 Wakker B.P., van Woerden H., 1991, *A&A*, 250, 509  
 Wakker B.P., van Woerden H., 1997, *ARA&A*, 35, 217  
 Welsh B.Y., Sfeir D.M., Sirk M.M., Lallement R., 1999, *A&A*, 352, 308  
 Welty D.E., Hobbs L.M., Kulkarni V.P., 1994, *ApJ*, 436, 152  
 Welty D.E., Morton D.C., Hobbs L.M., 1996, *ApJS*, 106, 533  
 White R.E., 1974, *A&A*, 31, 459

This paper has been typeset from a  $\text{\TeX}/\text{\LaTeX}$  file prepared by the author.